EPJ Photovoltaics **13**, 11 (2022)

https://doi.org/10.1051/epjpv/2022006

Available online at:
www.epj-pv.org

REGULAR ARTICLE OPEN ACCESS

Quantifying the performance gain of 100 cm^2 bifacial four terminal perovskite-Si tandem modules

Petra Manshanden[1,*], Gianluca Coletti[1], Victor Rosca[1], Mark J. Jansen[1], Koen de Groot[1], Gertjan J. de Graaff[1], M. Creatore[3], Lukas Simurka[2], Mehrdad Najafi[2], Valerio Zardetto[2], Ilkar Dogan[2], Henri Fledderus[2], and Sjoerd C. Veenstra[2]

[1] TNO Energy Transition, Westerduinweg 3, 1755 LE Petten, The Netherlands
[2] TNO Energy Transition, High Tech Campus 21, 5656 AE Eindhoven, The Netherlands
[3] Department of Applied Physics, Eindhoven University of Technology, P.O. Box 513, 5600 MB Eindhoven, The Netherlands

Received: 28 June 2021 / Received in final form: 4 February 2022 / Accepted: 3 March 2022

Abstract. Improving the performance of solar modules requires the implementation of both spectral and directional irradiance optimization. The performance of bifacial four-terminal tandem minimodules with a 100 cm^2 area is reported, both indoor and outdoor measurements. We demonstrate a 24.5 mW/cm^2 (bifacial irradiance 200 W/m^2) bifacial tandem power density, measured according to a tandem adapted IEC60904-1-2 protocol, which constitutes a 3 mW/cm^2 gain with respect to monofacial use. In addition, we show that in outdoor measurements bifacial four terminal tandems outperform identical monofacial four terminal tandems by 26% on average, depending on incident angle, injection level and temperature, in a 10% albedo environment. The average gain is higher for outdoor performance than for indoor performance, due to variations in relative rear irradiance.

Keywords: Four terminal tandem / bifacial modules / perovskite / outdoor performance

1 Introduction

In order to further reduce the Levelized Cost Of Electricity (LCOE) of PV, either costs, including installation and fees, need to come down or conversion efficiency must increase. As the photovoltaically active part of the installation constitute a minority of the total costs [1], improving the conversion efficiency for nearly the same costs is an effective route to lower LCOE. Ideally, the conversion efficiency should increase beyond the practical limit of silicon technology (26% [2]). It has been shown that tandem module technology, combining bottom c-Si cells with low-cost thin-film top cells, can overcome the theoretical limit for the efficiency of a single junction solar cell [3]. Recently, bifacial glass/glass modules are gaining market share because of the increased module power output of 10–20% from the rear illumination, depending on latitude [4]. In this concept, the glass-glass configuration gains one the assurance of long-term reliability in exchange for the added weight of the module. Therefore, the minimum efficiency target of tandem modules should consider the energy yield of bifacial c-Si modules as 'competition' and hence aim for power output densities >30 mW/cm^2. Additionally, tandem modules should demonstrate same reliability, bankability and competitive cost compared to commercial PV modules. Bifacial tandem modules combine the best of two worlds: tandem for better spectrum utilization, and bifaciality for highest module power [5,6].

Proper builds for tandems depend on correct spectral matching. Details on spectrally matching silicon with perovskite can be found elsewhere [7]. Decoupling the front and rear devices by using four terminal tandems has the added advantage that without current or voltage matching of the devices, the rear irradiance of the rear cell can be set to any desired value without increasing the current or voltage mismatch, which would impact the maximum power point [8].

In this paper we justify the use of bifacial tandem devices computationally and experimentally both indoors and outdoors in a rooftop laboratory by showing improved performance with respect to monofacial tandem devices. In addition, we show how the indoors measurement protocol (IEC60904-1-2) must be adapted to arrive at correct, comparable, and transferable parameters.

2 Method

2.1 Computational justification for bifacial tandem devices

Assuming equal efficiencies for top and bottom cell under standard test conditions (STC: 1000 W/m^2, AM1.5

* e-mail: petra.manshanden@tno.nl

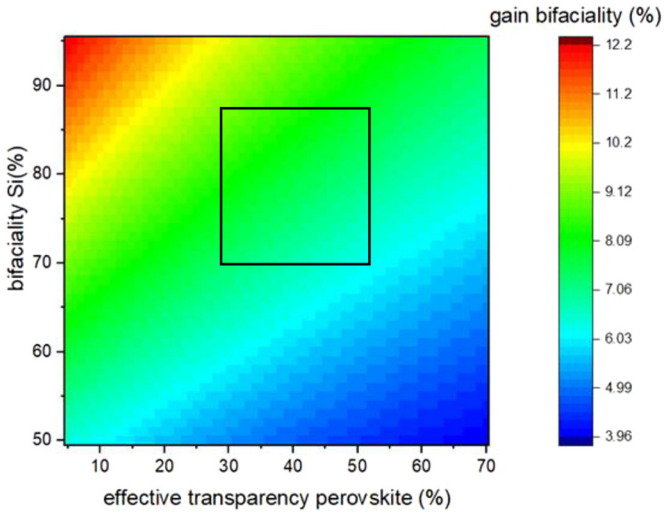

Fig. 1. Additional power (in percentages) due to the bifaciality of the bottom cell in comparison to the same tandem module applied monofacially assuming rear injection of 135 W/m^2 with STC front, and equal single junction device efficiencies at STC. The transparency of the perovskite is bottom cell efficiency/single junction efficiency ratio. The bifaciality of the silicon cell is for the silicon cell as component. This graph provides a visual representation of the justification of bifacial tandems. Note the square in the graph denotes common distribution of bifaciality and transmission.

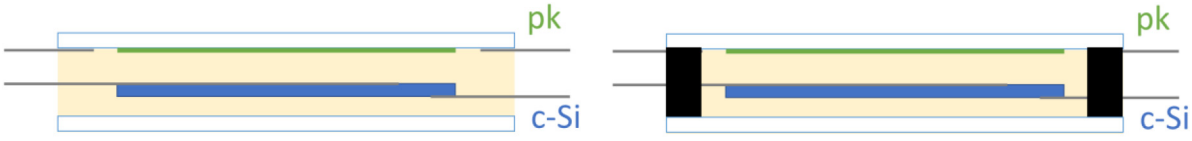

Fig. 2. Schematic pictures of the 100 cm^2 effective area bifacial 4T tandem device. Left: as used indoors; the edges are sealed by the encapsulant. Right: as used outdoors; additional sealing is applied around the contacts.

spectrum, 25 °C), the gain of a bifacial 4T tandem compared to an identical monofacial 4T tandem can be computed (see Fig. 1). Figure 1 computes the power gain for varying values of the bifaciality of the bottom silicon device and varying values for the effective transparency of the perovskite.

As the transparency of any object is a spectral graph, which is difficult to summarize in a single figure, the effective transparency is defined as the fraction of efficiency the bottom device will deliver in tandem configuration compared to standard test conditions. In the figure, the black square denotes the most common range of values, so the expected gain for 13% rear irradiance is 6–10%. This figure is slightly lower than for a silicon bifacial module since the power output due to front illumination is enhanced while the rear illumination part remained unchanged.

We note that the power gain is directly proportional to the bifacial irradiance in this simple simulation. Also, in case the STC power of the bottom device is significantly higher than of the top device, the power gain will be higher.

2.2 Device description

The schematic of the actual samples under consideration is shown in Figure 2. We used perovskite mini-modules fabricated on 6-inch substrates using scalable deposition methods (sputter coating, slot die coating and Atomic Layer Deposition (ALD) in combination with a laser scribed monolithic interconnection process. The 6-inch glass sheet features a fully interconnected 100×100 mm^2 perovskite minimodule, consisting of 31 monolithically interconnected cells with triple cation perovskite active layer as shown in [9,10]. Leads were affixed to the perovskite minimodule with conductive adhesive and copper tabs. Next, the semi-transparent mini-modules were encapsulated with the bottom bifacial PERC+ (Passivated Emitter Rear Cell) solar cells of industrial 6-inch (M2) size, laser cut to match the size of the perovskite modules. A commercial thermoplastic polyolefin (TPO) was used as encapsulant. The modules meant for outdoor testing had a commercial edge sealant applied before the main lamination step. One of the originally bifacial modules was made monofacial by covering the rear with black foil to mimic the conditions of bifacial indoor measurements.

The device parameters of the components of the 4T tandem are shown in Table 1. The perovskites were light-soaked for 7 min at maximum power point before measuring. Measurements were performed with a steady state AAA class solar simulator (Wacom) and calibrated IV tracers. Temperature was maintained at 25 °C with a thermostatic chuck and checked by a PT100 temperature sensor. Reference cells were spectrally matched to the devices.

Table 1. Device parameters of the components of the 4T tandem devices. All devices are 100 cm^2 at the time of measurement.

	Perovskite (forward)	Perovskite (reverse)	PERC+ (monofacial)
I_{sc} (A)	0.0632	0.0624	3.99
V_{oc} (V)	33.17	33.25	0.684
FF (%)	70.6	73.1	79.0
Efficiency (%)	14.8	15.2	21.5
Bifaciality (%)			69

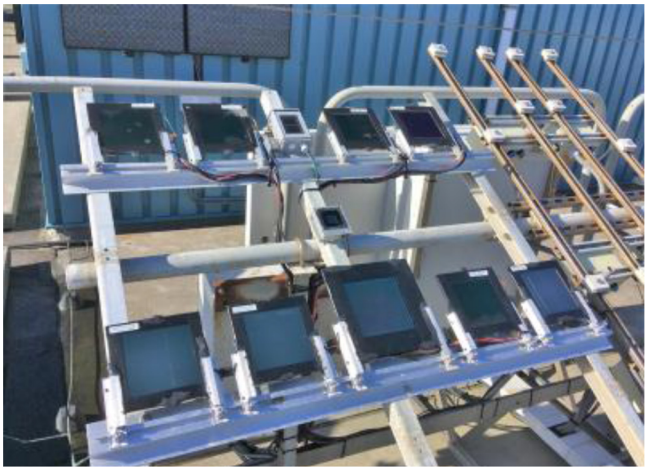

Fig. 3. Photograph of outdoor facility. Top row was assigned to this experiment.

From these device parameters, using the simple model in the previous paragraph, we estimate at a rear irradiance of 135 W/m^2 a gain for this tandem device due to bifaciality of 8.9%.

2.3 Outdoor measurement setup

For outdoor measurements we employed our rooftop outdoor facility facing south at an angle of 30 degrees at 100 cm from the background, which has 10% albedo (see Fig. 3). The rooftop outdoor facility has been introduced in [11]. The devices were monitored by PT100 temperature sensors and silicon monitor cells in plane with the tandems facing front and rear. The monitoring time was 18-12-2020 to 30-5-2021, the monitoring frequency was every 10 minutes with IV sweeps of 10 s, and the location was Petten, the Netherlands. In-between measurements, all samples were kept at the last measured maximum power point.

2.4 Indoor measurement protocol

2.4.1 Justification of the adaptation

As mentioned in the scope of the IEC60904-1-2 [12] standard, it is only applicable to single junction devices and modules. Hence, for our purposes, the standard is not applicable. However, the standard principle can be used as a foundation to create an applicable measurement protocol, which is the goal here.

According to the standard IEC60904-1-2, bifacial performance can be assessed indoors (paragraph 6.3 of the standard) by either bifacial illumination or single sided illumination from the front. While bifacial illumination can be applied without modifications, the protocol for the single sided illumination has some issues due to breached assumptions.

A perovskite which is active over most of the visual spectrum used as top device will leave less than 60% of the photons available for power conversion by the bottom device, and in practice fewer. If the bottom cell has a better bifaciality than 60% (current commercial values are 70–80%), at STC rear performance from the bottom cell will be higher than the front performance. Assuming a current decrease of 35% due to filtering by the top device, and a commercially typical bifaciality of 70%, the necessary additional front injection is approximately 150%. This is outside the range of standard non-concentrator solar simulators, which typically have an upper range less than 130% (1300 W/m^2).

2.4.2 Adapted protocol

As the rear cell is filtered when the tandem device is illuminated from the front side, the spectral response of the rear device is known to be significantly different when measured from the front and the rear due to the spectrally heterogeneous filtering of the perovskite (see Fig. 4). Therefore, correction of the spectral mismatch cannot be neglected, and it is advisable to use spectrally matched references for each application.

In contrast to the protocol of the IEC standard, the light injection needs to be lowered by a significant fraction instead of raised slightly as the bottom cell works at a fraction of STC power at monofacial illumination. As mentioned before, solar simulators typically do not have the capability to do this while staying within A class, and therefore neutral density filters are applied. However, while the lamp power can be adjusted continuously, a neutral density filter is an object with fixed transparency and is supplied as finite set. However, a judicious combination of lamp power and filtering can achieve a wide variety of illumination levels. In addition, the standard allows for an accuracy of 10% in reaching the desired irradiance level, and correction to the desired level by translating the IV curve (application of IEC 60891 [12]). This protocol is summarized in the flowchart of Figure 5.

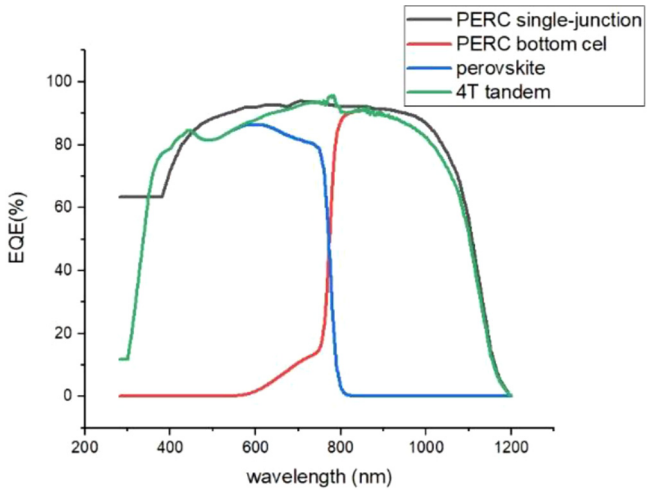

Fig. 4. External Quantum Efficiency (EQE) graphs of the PERC and perovskite components, and their combination.

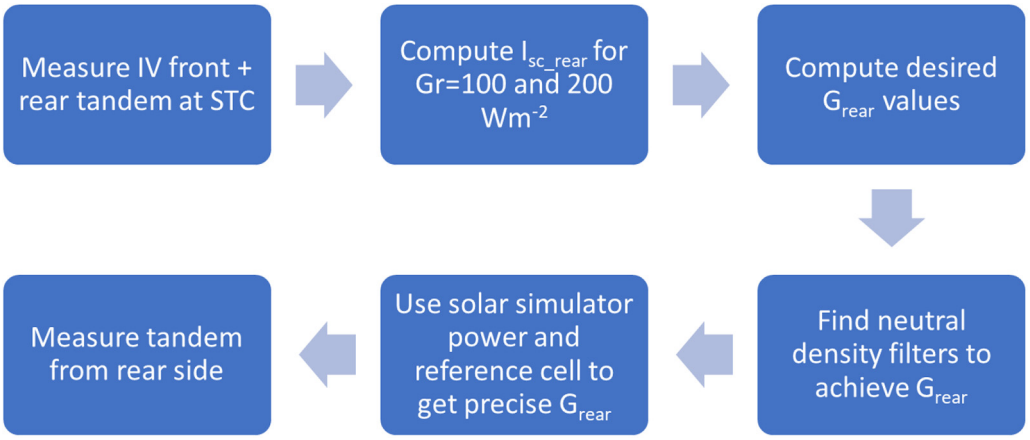

Fig. 5. Flow chart of adapted protocol as proposed in paragraph.

3 Results

3.1 Application of the protocol

For full four terminal performance, the performance of the front side is added to the rear side, separately for each rear injection as shown in Table 2.

We show a gain of 8.4% relative for a rear injection of $100\,\mathrm{W\,m^{-2}}$, and a gain of 14% relative for a rear injection of $200\,\mathrm{W\,m^{-2}}$. This is reasonably close to the outcome of our computed simplified model.

We show a gain of 0.9 $\mathrm{mWcm^{-2}}$ for monofacial tandem, and a gain of 1 $\mathrm{mWcm^{-2}}$ for bifacial tandem, with a reproducibility on power of less than 0.03 $\mathrm{mWcm^{-2}}$ as assessed for silicon devices. This difference between monofacial and bifacial for PERC as bottom and as single device is caused by two factors. Firstly, the contribution from the rear is higher for the 4T tandem construction compared to the single junction device because of the filtering by the perovskite top cell . Secondly, the loss due to series resistance in the PERC+ component is much higher for the single junction devices than for the 4T tandem configuration. In fact, for the 4T situation, bifacial application leads to no FF loss, whereas solitary application leads to ∼1% FF loss. The reason for this is that the (commercial) solar cell has been designed to carry currents of >10 A which will not occur in tandem applications.

3.2 Outdoor performance

Identical 4T tandems were placed in our rooftop outdoor facility as described in the methods section. One of the devices was made monofacial by applying a black rear at the time of module manufacturing, which ensured all differences found in the data were due to the bifaciality and not manufacturing differences of the silicon device. In these circumstances and measurement period, the power gain of a bifacial module compared to a bifacial module made monofacial is on average 26.2%.

Over the entire runtime of the experiment, the temperature of the monofacial device was on median $0.23 \pm 0.55\,^{\circ}\mathrm{C}$ higher than the bifacial device. This difference in temperature has some effect on the electrical

Table 2. Cell and module efficiency of our 4T bifacial tandems with aperture area of 100 cm^2.

		Cell power density (mW/cm^2)	4T power density (mW/cm^2)
Perovskite	Forward scan	14.8	
	Reverse scan	15.2	
PERC+ not filtered	Monofacial	20.6	
	Bifacial $G_{rear} = 100\ Wm^{-2}$	22.0	
	Bifacial $G_{rear} = 200\ Wm^{-2}$	23.5	
PERC+ filtered	Monofacial	6.8	21.4
	Bifacial $G_{rear} = 100\ Wm^{-2}$	8.6	23.2
	Bifacial $G_{rear} = 200\ Wm^{-2}$	9.9	24.5

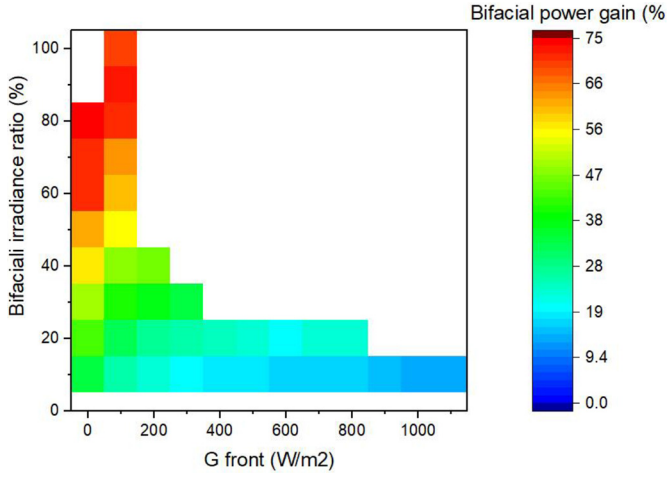

Fig. 6. Dependency of the bifacial gain to the bifacial and front irradiance. The roof on which the devices were installed has an albedo of ~10%. The irradiance at the rear of the tandem devices is never less than 5% of the irradiance at the front of the devices. The high values of bifacial irradiance ratio and irradiance can be explained by local effects of the apparent yearly solar movement. Note that the photovoltaic data is not temperature corrected, and data with an incidence less than 5 times is omitted.

parameters, but the observed effects are clearly larger than could be explained by temperature effects [13,14].

The dependency of the bifacial gain compared to an identical monofacial device is depicted in Figure 6. The bifacial gain is defined as the increase of performance of a bifacial device relative to an identical monofacial device. The bifacial irradiance ratio is the fraction of light incident at the rear, with respect to the front irradiation at that time. Only data with stable front side illumination above $2\,W/m^2$ is used. The data was binned, and bins containing fewer than 5 occurrences are not shown. Note that 85% of the data corresponds to a bifacial irradiance ratio of approximately 10%. Also note that the bifacial irradiance ratio axis was clipped at 110% for reasons of graph clarity while data with much higher bifacial irradiance ratio was available (all at irradiance levels $<200\,W/m^2$).

Smaller variations in bifacial irradiance ratios, especially at lower irradiance levels, can be explained by the relatively high incidence of diffuse light due to prevalent weather conditions in the Netherlands.

The very high bifacial irradiance ratios can be explained by the movement of the sun relative to the location the modules were placed at. In spring and summer, the sun rises in the north-east in Petten, and sets in the north-west, which means that for south facing fixed modules at times the primary irradiation will occur at the rear of the modules. Similarly for high front irradiances, while the average unclouded irradiance over the year in Petten will be approximately AM1.5, at noon during the summer the irradiance will be closer to AM1 than to AM1.5. Also, the larger surroundings of the location contain some reflective surfaces (other buildings, the sea), which increase the maximum irradiance as well.

The reason for the lower magnitude variability of the bifacial irradiance ratio of the setup is that cloudy weather causes diffuse irradiance. Diffuse irradiance lowers the front irradiance significantly, but rear irradiance is reduced by a smaller fraction, thereby increasing the profit gained from bifaciality of modules.

As can be seen from Figure 6, the bifacial gain is strongly injection dependent, with higher gain for lower irradiances. This is shown more clearly in the temperature-irradiance dependency in Figure 7. In addition, this graph also shows that for higher temperatures the bifacial power gain of the 4T tandem is lower than for lower temperatures for the same irradiance. This is caused by a stronger temperature dependency of the silicon in comparison to the perovskite [13,14].

A second notable point seen in Figure 7 is the high variability of the bifacial power gain with the $0–50\,W/m^2$ irradiance for different temperatures. The reason for this high variability is that this line encompasses a large variety of outdoor conditions, from a snow-covered roof in winter to sunrise during a bright morning in late spring and everything in between. This point is illustrated in Figure 8, where we show the bifacial irradiance ratio over the year with notes concerning the weather and solar position. Notable periods are a snow period, and the astronomical spring and summer. During the snow period, the power gain due to bifaciality was 60 mW, or about 40% at times of full snow cover. As the snow ages and melts, the relative power gain decreases. Also, at the location of measuring, the sun rises and sets to the north in spring and summer.

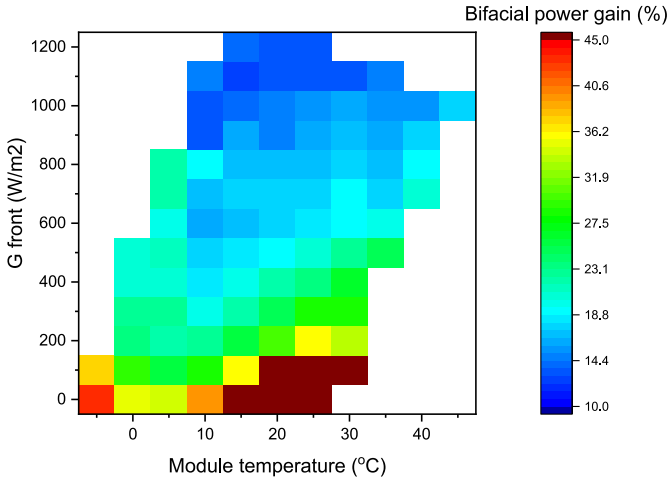

Fig. 7. Temperature-irradiance dependency of the bifacial power gain. For higher irradiances, bifacial power gain is less. For higher temperatures, the bifaciality is less as well. The lower bifacial power gain for higher irradiances is caused in the midrange by weather conditions, and in the lower range by the changing solar angles. The lower gain for higher temperatures is caused by the higher temperature dependency of the bifacial rear device as compared to the front device. The gain of high temperature low irradiance is very high as that is caused by northern sunset/sunrise.

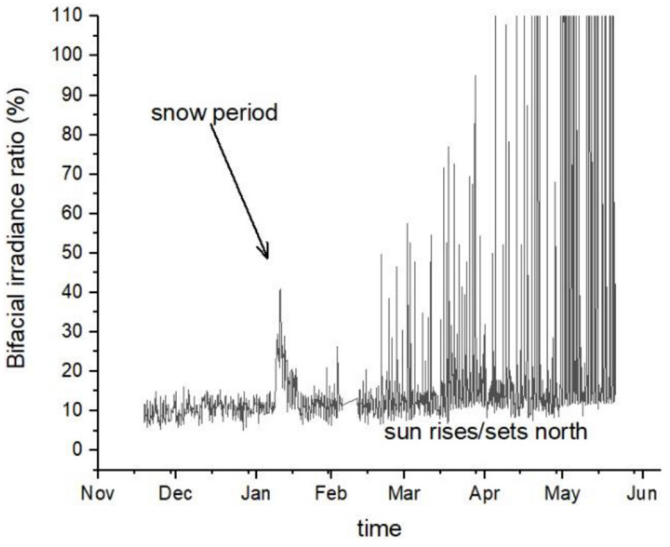

Fig. 8. Bifacial irradiance ratio at our location over the reported time period. The period in which it snowed is easily found in the irradiance data (indicated by arrows). Starting at the astronomical spring, the bifacial irradiance increases at sunrise and sunset. The maximum bifacial irradiance ratio can reach up to 500 % for clear weather when nearing the onset of summer.

Therefore, each day the sun rises and sets behind the modules, causing most of the irradiance to come from the rear, and hence the bifacial irradiance radio to rise above 100%.

3.3 Comparison of indoor to outdoor performance

As the ultimate justification for indoor measurement is to establish an estimation of eventual outdoor performance, it is useful to compare indoor and outdoor results in order to establish the accuracy of the predictor measurement [e.g. 11,15,16]. A direct comparison at approximately 1000 W/m^2 is shown in Figure 9, which is analogous to graph 4 of IEC60904-1-2. The module temperature varies in that time from 5 to 39 °C and 436 points were selected.

Even though we are comparing indoor measurements with controlled irradiation levels and controlled temperature to outdoor measurements in which both have a far wider range, the correspondence is well within the $k = 2$ uncertainty level as assessed from the 436 datapoints of outdoor measurements. Not stated in the graph is the uncertainty in the indoor measurement setup of 1.9% relative, which is dominated by the systematic uncertainty of the reference cell. This proves that the proposed procedure provides us with an accurate estimate of outdoor performance.

4 Discussion

In Figure 1 we estimated theoretically the gain a bifacial 4T module may expect in a variety of builds. In our case,

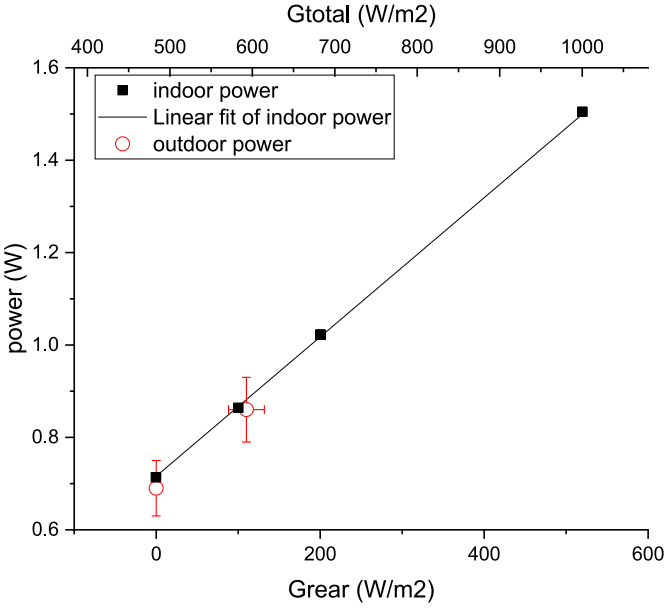

Fig. 9. Outdoor performance compared to indoor performance at 1000 W/m^2 of the rear component only. G_{rear} is the additional rear irradiance. G_{total} is the corresponding total irradiance from the rear only to achieve the necessary injection level. The module temperature is uncontrolled and varies between 5 and 39 °C, due to outdoor temperature variations between 2 and 21 °C. The error bars are at $k = 2$ of all measurement data points. Approximately 400 datapoints are contained in each outdoor data point.

we would expect a gain of 6.8% for a rear irradiance of 135 W/m^2, with a front irradiance of 1000 W/m^2. Over the entire measurement period we have found a bifacial power gain of 26.2%. This disparity can be explained by the higher bifacial irradiance ratio especially at lower irradiance levels caused by solar angles and diffuse irradiance. Restraining oneself to approximately the same irradiance conditions outdoors, we read out a bifacial gain of 10.2%. Given the variability of the rear injection and the variability in temperature, this is reasonably close to the computed and indoor values.

In order to correctly assess the bifaciality of a four terminal device in a monofacial setup, some amendments to IEC 60904-1-2 have to be made. This involves irradiance from the rear up to a total current equal to the current from the front (filtered) added to the current of the desired rear irradiance. This sum will be typically less than the STC rear current. Achieving this current without affecting the spectrum can be realized by filtering the rear cell with neutral density filters. Any remaining deviations from the desired current can be further matched by slight changes in the lamp settings and if necessary finetuning by translating the IV curve.

In contrast to the theoretical findings of Chantana et al. [3], in our outdoor data it is shown that bifacial performance is difficult to estimate from the albedo the total gain due to the bifacial irradiance ratio. Because of solar angles and weather conditions, the albedo provides us with a number closer to the minimum bifacial irradiation ratio, and hence indoor estimated performance gain is most of the time a minimum gain.

We observed that 15% of the daylight time, the bifacial irradiation ratio does not correspond to the albedo of the surroundings. The variability of actual bifacial illumination ratio during the approximate half year of measuring also indicates a problem with the application of bifaciality to two terminal tandems. While it is eminently possible to optimize a tandem device with a particular bifacial irradiation ratio in mind, variable bifacial irradiation ratios cannot be optimized for. The variable rear irradiation causes a variable relative current from the bottom device, which causes a current mismatch between the top and bottom cell. This mismatch drives both subcells out of their maximum power point, which means it loses part of the potential power gain. This effect is more severe for current matched two terminal tandem devices than for voltage matched two terminal tandem devices because the voltage changes with irradiation logarithmically instead of linearly as for current.

5 Conclusions

We computed that 4T tandems with 13.5% bifacial illumination added can expect over 6% power gain for identical power top and bottom devices at STC. For lower bifacial illumination ratios, the gain is proportionally lower. For relatively more powerful bottom devices, the gain will be proportionally higher. We show that for our devices, placed at a ∼10% albedo site, we see an average gain due to bifacial irradiance of 26% over which is significantly higher than computed. This is explained by the experimental finding that outdoors the bifacial irradiance ratio is not a fixed number but subject to change due to weather and solar angles. It is noted in the discussion that the variable bifacial irradiance ratio produces some issues for 2T bifacial devices.

We proposed a variation on the IEC60904-1-2 standard to enable bifacial measurement on 4T tandem devices. This was verified by comparing indoor data according to the standard to outdoor data with sufficiently corresponding outdoor conditions.

This research received no external funding.

Author contribution statement

Conceptualization: PM, GC; Methodology: PM; Validation: PM; Investigation: PM, MJ, KG, GG; Resources: LS, MN, VZ, ID, HF, SV and MC; Writing – Original Draft: PM; Writing – Review and Editing: GC, VR; Visualization: PM; Supervision: GC, SV; Project Administration: GC.

References

1. European Commission, Joint Research Centre, A. Jäger-Waldau, PV status report 2019, Publications Office, 2019, https://data.europa.eu/doi/10.2760/326629
2. R.M. Swanson, Approaching the 29% limit efficiency of silicon solar cells, in Conference Record of the Thirty-first IEEE Photovoltaic Specialists Conference, 2005
3. S. Kim, T.T. Trinh, J. Park et al., Over 30% efficiency bifacial 4-terminal perovskite-heterojunction silicon tandem solar cells with spectral albedo, Sci. Rep. **11**, 15524 (2021)
4. C.D. Rodríguez-Gallegos, M. Bieri, O. Gandhi, J. Prakash Singh, T. Reindl, S.K. Panda, Monofacial vs bifacial Si-based PV modules: which one is more cost-effective? Solar Energy **176**, 412 (2018)
5. G. Coletti et al., Bifacial four-terminal perovskite/silicon tandem solar cells and modules, ACS Energy Lett. **5**, 1676 (2020)
6. J. Chantana, Y. Kawano, T. Nishimura, A. Mavlonov, T. Minemoto, Optimized bandgaps of top and bottom subcells for bifacial two-terminal tandem solar cells under different back irradiances, Solar Energy **220**, 163 (2021)
7. S.L. Luxembourg, D. Zhang, M. Najafi et al., Perovskite/Crystalline silicon tandems: impact of perovskite bandgap and crystalline silicon cell architecture, in 33rd EUPVSEC 2017, https://doi.org/10.4229/EUPVSEC20172017-3DV.2.70
8. M.H. Futscher, B. Ehrler, Efficiency limit of Perovskite/Si tandem solar cells, ACS Energy Lett. **1**, 863 (2016)
9. D. Zhang, M. Najafi, V. Zardetto et al., High efficiency 4-terminal perovskite/c-Si tandem cells, SEM&SC **1880**, 1 (2018)
10. V. Zardetto et al., Towards large area stable perovskite solar cells and modules, in 48th IEEE PVSEC 2019, https://doi.org/10.1109/pvsc40753.2019.8981217

11. B.B. Van Aken, M.J. Jansen, A.J. Carr, G.J.M. Janssen, A.A. Mewe, Relation between indoor flash testing and outdoor performance of bifacial modules, in Proceedings of the 29th European Photovoltaic Solar Energy Conference (2014), pp. 2399–2402
12. www.iec.ch
13. S. Ponce-Alcantara, G. Sanchez, J.P. Conelly, J.M.M. Novoa, A statistical analysis of the temperature coefficients of industrial silicon solar cells, Energy Procedia **55**, 578 (2014)
14. L. Lin, N.M. Ravindra, Temperature dependence of CIGS and perovskite solar cell performance: an overview, SN Appl. Sci. **2**, 1361 (2020)
15. A. Virtuani, H. Mullejans, E.D. Dunlop, Comparison of indoor and outdoor performance measurements of recent commercially available solar modules, Progr. Photovolt. **19**, 11 (2010)
16. C. Deline, S. Macalpine, B. Marion, F. Toor, A. Asgharzadeh, J.S. Stein, Assessment of bifacial photovoltaic module power rating methodologies-inside and out, IEEE J. Photovolt. **7**, 575 (2017)

Cite this article as: Petra Manshanden, Gianluca Coletti, Victor Rosca, Mark J. Jansen, Koen de Groot, Gertjan J. de Graaff, M. Creatore, Lukas Simurka, Mehrdad Najifi, Valerio Zardetto, Ilkar Dogan, Henri Fledderus, Sjoerd C. Veenstra, Quantifying the performance gain of 100 cm^2 bifacial four terminal perovskite-Si tandem modules, EPJ Photovoltaics **13**, 11 (2022)